12-2-2022

On a Guiding of Whistler-Mode Waves by Density Gradients

Anatoly V. Streltsov
Embry-Riddle Aeronautical University, streltsa@erau.edu

On a Guiding of Whistler-Mode Waves by Density Gradients

Anatoly V. Streltsov[1]

[1]Department of Physical Sciences, Embry-Riddle Aeronautical University, Daytona Beach, FL 32114, USA

Key Points:

- Localized packages of VLF whistler-mode waves are frequently observed by satellites in the vicinity of density gradients.
- We model the guiding of these waves by the density gradients using equations of electron magnetohydrodynamics.
- We show that the whistler-mode wave can be guided by plasma gradients with a size less than the characteristic transverse size of the wave.

Corresponding author: A.V. Streltsov, streltsa@erau.edu

Abstract

Observations from satellites demonstrate that in the magnetosphere, VLF whistler-mode waves are frequently detected in the narrow transition regions, where the plasma density changes its magnitude over a short distance across the ambient magnetic field. These observations suggest that the small-scale, isolated density gradients can guide the VLF whistler-mode waves along the field. We investigate the guiding of the whistler-mode waves by the transverse density gradients with a size much less than the characteristic perpendicular size of the wave. We found analytical solutions describing these waves in the plasma with a sharp density discontinuity between two homogeneous regions, and confirm with time-dependent, two-dimensional simulations that these waves are indeed guided by the discontinuity. Simulations also reveal that the parameters of the guided waves (the frequency and parallel wavelength) relate to the parameters of the plasma.

1 Introduction

Observations by NASA Van Allen Probes satellites (also known as Radiation Belt Substorm Probes or RBSP) reveal that in the equatorial magnetosphere small-scale, localized packages of VLF waves frequently correlate with inhomogeneities of the background plasma density. These inhomogeneities may have different shapes: They can be formed by the density depletion, enhancement, single density gradient (or a transition layer between two homogeneous regions), and density "shelf." But their size and location always correlate with the size and location of the wave packages [*Ke et al.*, 2021; *Chen et al.*, 2021a; *Streltsov*, 2021a,b].

Figure 1a shows an example of the observations showing small-scale packages of VLF waves and density structures. It shows the plasma density and the power spectral density (PSD) of the electric field measured by the RBSP-B satellite on 2016-02-27 from 18:26 to 18:45 UT. During this time interval, the satellite was in the equatorial plane (MLat $\approx -6.3°$) at the radial distance of $\approx 4.2\ R_E$.

The Van Allen Probes satellites measure the electric field, magnetic field, and plasma density by the Electric Field and Wave (EFW) instrument [*Wygant et al.*, 2013] and the Electric and Magnetic Field Instrument Suite and Integrated Science (EMFISIS) instrument [*Kletzing et al.*, 2013]. The measurements are taken in the (u, v, w) satellite coordinate system, where the w axis is co-aligned with the satellite spinning axis. The VLF wave activity is clearly seen in all three components of the electric field, and in this paper, we use the E_w only to illustrate the main features of the observed waves.

Due to the high parallel mobility of the electrons, it is reasonable to assume that the observed density inhomogeneities extend along the ambient magnetic field forming channels or ducts. The channel where the density inside is greater than outside is called a high-density duct, and the channel formed by the density depletion is called a low-density duct. These ducts are frequently observed in space and laboratory plasmas, and they are studied in depth. Comprehensive reviews of theory and observations related to the VLF waves inside high-density and low-density ducts with a relatively symmetric, Gaussian-like density profile across the magnetic field are given by *Helliwell* [1965]; *Sazhin* [1993]; *Kondrat'ev et al.* [1999].

Figure 1a demonstrates that whistler-mode waves can be guided/ducted in the magnetosphere by the field-aligned density homogeneities with every possible structure. As a result, it may be hard, or even impossible to identify exactly the region where the waves registered by the satellite are generated. This study focuses on the whistler-mode waves guided by a single transverse density gradient. Three examples of localized packages of these waves observed by the RBSP-B satellite on a narrow density gradient are shown in Figures 1b, 1c, and 1d.

- Figure 1b shows the event occurring at 18:37:26 UT. At this time, $B_0 = 437.8$ nT, $n_0 = 631.7$ cm^{-3}, the electron cyclotron frequency $\omega_{ce} = 7.71 \times 10^4$ rad/s, the electron plasma frequency $\omega_{pe} = 1.42{\times}10^6$ rad/s, and the lower-hybrid frequency $\omega_{LH} = 1.80 \times 10^3$ rad/s.
- Figure 1c shows three events. The first event occurs at 18:40:49 UT. At this time, $B_0 = 416.5$ nT, $n_0 = 576.0$ cm^{-3}, $\omega_{ce} = 7.44 \times 10^4$ rad/s, $\omega_{pe} = 1.35 \times 10^6$ rad/s, and $\omega_{LH} = 1.71 \times 10^3$ rad/s. The second event occurs at 18:41:02 UT. At this moment, $B_0 = 415.5$ nT, $n_0 = 576.0$ cm^{-3}, $\omega_{ce} = 7.31{\times}10^4$ rad/s, $\omega_{pe} = 1.35 \times 10^6$ rad/s, and $\omega_{LH} = 1.71 \times 10^3$ rad/s. And the third event occurs at 18:41:26 UT. At this moment, $B_0 = 412.3$ nT, $n_0 = 576.0$ cm^{-3}, $\omega_{ce} = 7.26 \times 10^4$ rad/s, $\omega_{pe} = 1.35 \times 10^6$ rad/s, and $\omega_{LH} = 1.69 \times 10^3$ rad/s.
- Figure 1d shows two events. One event occurs at 18:43:52 UT. At this time, $B_0 = 398.3$ nT, $n_0 = 523.0$ cm^{-3}, $\omega_{ce} = 7.01 \times 10^4$ rad/s, $\omega_{pe} = 1.29 \times 10^6$ rad/s, and $\omega_{LH} = 1.64 \times 10^3$ rad/s. The second event occurs at 18:44:25 UT. At this

time, $B_0 = 395.4$ nT, $n_0 = 523.0$ cm^{-3}, $\omega_{ce} = 6.96 \times 10^4$ rad/s, $\omega_{pe} = 1.29 \times 10^6$ rad/s, and $\omega_{LH} = 1.62 \times 10^3$ rad/s.

Studies by *Inan and Bell* [1977]; *Woodroffe and Streltsov* [2013]; *Streltsov* [2021a]; *Chen et al.* [2021b] demonstrate that whistler-mode waves can be guided along the magnetic field by the combined effect of transverse gradients in the density and the ambient magnetic field. This mechanism works in relatively large-scale ducts where the magnitude of the ambient magnetic field changes substantially over the duct width. These are so-called "wide" ducts, which are not considered in this study.

When the density gradient occurs over a relatively small distance across the field, like in the events illustrated in Figures 1b - 1d, the variation in the magnetic field can be neglected, and the mechanism describing "wide" ducts is not applicable. *Streltsov et al.* [2006] consider the guiding of whistler-mode waves by the density gradient with a size small enough so that the inhomogeneity of the background magnetic field can be ignored, but larger than the perpendicular wavelength of the guided wave. That ducting mechanism stops working when the perpendicular wavelength is comparable or less than the characteristic size of the density inhomogeneity. The goal of this study is to investigate the guiding of whistler-mode waves by the density inhomogeneities with transverse sizes less than the characteristic perpendicular size of the wave. This goal will be achieved via analytical and numerical investigation of the electron-magnetohydrodynamics (EMHD) model describing VLF whistler-mode waves in the inhomogeneous magentospheric plasma.

2 Model

In all these events shown in Figures 1b - 1d, PSD of E_w reaches its maximum at the frequency $f = 450$ Hz corresponding to $\omega = 2.83 \times 10^3$ rad/s. And in all events ω, ω_{ce}, ω_{pe}, and ω_{LH} satisfy the conditions

$$\omega_{LH} < \omega < \omega_{ce} \ll \omega_{pe}. \tag{1}$$

Sazhin [1993] demonstrates that when the conditions (1) are satisfied, the dynamics of VLF whistler-mode waves can be described with a so-called quasi-longitudinal electron-MHD model. This model assumes that ions are immobile (because of $\omega_{LH} < \omega$) and electrons can be treated as a cold fluid [*Helliwell*, 1965; *Gordeev et al.*, 1994]. Because ions are immobile and the plasma is quasi-neutral, the density continuity equation for electrons is omitted, and the model consists of the electron momentum equation and the Maxwell equations only.

The displacement current is omitted in the Ampere's law and this is the essence of the "quasi-longitudinal" approximation. Initially it was developed for the waves propagating under a small angle to the ambient magnetic field. Later, it was shown in several monographs (e.g. [*Helliwell*, 1965; *Sazhin*, 1993]) that it is valid for almost any angle of wave propagation if the conditions (1) are satisfied.

The EMHD model, considered in this paper, consists of three vector equations for $\mathbf{E}$, $\mathbf{B}$, and the electron velocity, $\mathbf{v}$ [*Streltsov*, 2021a]:

$$\frac{m_e}{\mu_0 n e^2}\nabla\times\nabla\times\mathbf{E}+\mathbf{E} = -\frac{m_e}{e}(\mathbf{v}\cdot\nabla)\mathbf{v}-\mathbf{v}\times\mathbf{B} \quad (2)$$

$$\frac{\partial\mathbf{v}}{\partial t} = \frac{1}{\mu_0 n e}\nabla\times\nabla\times\mathbf{E} \quad (3)$$

$$\frac{\partial\mathbf{B}}{\partial t} = -\nabla\times\mathbf{E} \quad (4)$$

In the homogeneous media, the linearized equations (2)-(4) give the dispersion relation

$$k^2-\frac{\omega_{ce}}{\omega}k_\parallel k+\frac{\omega_{pe}^2}{c^2}=0. \quad (5)$$

Here, $k_\perp$ and $k_\parallel$ are magnitudes of components of the wave-vector $\mathbf{k}$ in the directions perpendicular and parallel to the background magnetic field $\mathbf{B}_0$.

Relation (6) can be used to express $k_\perp$ as

$$k_{\perp_{1,2}}=k_\parallel\left[\frac{\omega_{ce}^2}{4\omega^2}\left(1\mp\sqrt{1-\frac{n}{n_2}}\right)^2-1\right]^{1/2}, \quad (6)$$

where

$$n_2=k_\parallel^2\frac{m_e}{\mu_0 e^2}\left(\frac{\omega_{ce}}{2\omega}\right)^2. \quad (7)$$

Expression (7) shows that for some particular values of ω_{ce}, ω, and $k_\parallel$ there is no real $k_\perp$ in the plasma with $n>n_2$. In other words, the VLF wave with some particular ω and $k_\parallel$ cannot propagate in the direction perpendicular to $\mathbf{B}_0$, if $n>n_2$.

Let us find out how such waves look in the plasma with a small-scale density gradient (discontinuity) in the direction perpendicular to $\mathbf{B}_0$. We will study this problem in Cartesian, orthogonal coordinate system (x, y, z), where z directs along the ambient magnetic field. The background magnetic field is assumed to be uniform. The plasma density is uniform in the y and z directions and non-uniform in x. To simplify our analysis, we will consider this problem in two spatial dimensions, assuming that all $\partial/\partial y\equiv$

0. At the same time, each vector quantity considered here has all three vector components.

We consider the small-amplitude waves only and restrict our analysis with a linearized set of equations (2)-(4). In the linear case, equations (2) and (3) decouple from the equation (4) and, after some algebra, they can be reduced to one equation for $\mathbf{E}$ and $\dot{\mathbf{E}} = \partial \mathbf{E}/\partial t$:

$$\nabla \times \nabla \times \dot{\mathbf{E}} + \frac{\omega_{pe}^2}{c^2}\dot{\mathbf{E}} = -\omega_{ce}\left(\nabla \times \nabla \times \mathbf{E}\right) \times \hat{\mathbf{z}} \tag{8}$$

In the two-dimensional case, the vector equation (8) can be written as system of three scalar equations for E_x, E_y, and E_z:

$$\begin{aligned} \partial_{xz}\dot{E}_z - \partial_{zz}\dot{E}_x + \frac{\omega_{pe}^2}{c^2}\dot{E}_x &= \omega_{ce}\left(\partial_{xx}E_y + \partial_{zz}E_y\right) && (9)\\ -\partial_{xx}\dot{E}_y - \partial_{zz}\dot{E}_y + \frac{\omega_{pe}^2}{c^2}\dot{E}_y &= \omega_{ce}\left(\partial_{xz}E_z - \partial_{zz}E_x\right) && (10)\\ \partial_{xz}\dot{E}_x - \partial_{xx}\dot{E}_z + \frac{\omega_{pe}^2}{c^2}\dot{E}_z &= 0 && (11) \end{aligned}$$

We are looking for the waves propagating in the z direction and localized in x. In general form, the components of the electric field in such waves can be written as

$$E_x(x,z,t) = E_x(x)\sin(\phi), \quad E_y(x,z,t) = E_y(x)\cos(\phi), \quad E_z(x,z,t) = E_z(x)\cos(\phi), \tag{12}$$

where $\phi = k_z z - \omega t$. For these components, equations (9)-(11) can be rewritten as:

$$\begin{aligned} k_z\partial_x E_z - \left(k_z^2 + \frac{\omega_{pe}^2}{c^2}\right)E_x &= \frac{\omega_{ce}}{\omega}\left(\partial_{xx} - k_z^2\right)E_y && (13)\\ \partial_{xx}E_y - \left(k_z^2 + \frac{\omega_{pe}^2}{c^2}\right)E_y &= \frac{\omega_{ce}}{\omega}\left(k_z\partial_x E_z - k_z^2 E_x\right) && (14)\\ \partial_{xx}E_z - \frac{\omega_{pe}^2}{c^2}E_z - k_z\partial_x E_x &= 0 && (15) \end{aligned}$$

Equations (13) and (14) show that $E_x(x)$ can be found from $E_y(x)$ as

$$E_x(x) = \frac{\omega}{\omega_{ce}}\left[\frac{c^2}{\omega_{pe}^2}\left(\frac{\omega_{ce}^2}{\omega^2} - 1\right)\left(k_z^2 - \partial_{xx}\right) - 1\right]E_y(x). \tag{16}$$

After that, $E_z(x)$ can be found from $E_x(x)$ as a solution for equation (15). If $E_x(x)$, $E_y(x)$, and $E_z(x)$ are determined, then equations (3) and (4) can be used to find $\mathbf{v}(x)$ and $\mathbf{B}(x)$. Thus, $\mathbf{E}$, $\mathbf{B}$, and $\mathbf{v}$ will be determined, if we determine (or specify) $E_y(x)$.

Let us consider a plasma with a sharp density discontinuity in the x direction: $n = n_{01}$ when $x < 0$, and $n = n_{02}$ when $x \geq 0$. We will consider the wave with such ω

and $k_\parallel$, that $n_2 < \min\{n_{01}, n_{02}\}$. In this case, relation (6) tells us that a localized solution for $E_y(x)$ can be found as a function

$$E_y(x) = \begin{cases} E_{y1} \sin(\kappa_1 x)\, e^{\gamma_1 x}, \text{ if } x < 0 \\ E_{y2} \sin(\kappa_2 x)\, e^{-\gamma_2 x}, \text{ if } x \geq 0 \end{cases} \tag{17}$$

Here, $\kappa_{1,2} = \Re(k_\perp)$ and $\gamma_{1,2} = \Im(k_\perp)$ in the plasma with the density n_{01} and n_{02} correspondingly. $E_y(x)$ defined by (15) is a continuous function. Equation (13) shows that $E_x(x)$ is also continuous if $\partial_{xx}E_y(x)$ is continuous. The last condition is satisfied if $E_{y2} = -(\kappa_1\gamma_1/\kappa_2\gamma_2)E_{y1}$.

Figures 2a, 2b, and 2c show plots of $E_x(x)$, $E_y(x)$, $E_z(x)$ for the wave with $f =$ 450 Hz and $\lambda_\parallel = 33.0$ km in the uniform magnetic field $B_0 = 437.8$ nT and plasma with a density discontinuity at $x = 0$: $n_{01} = 695.5$ cm^{-3} and $n_{02} = 200.0$ cm^{-3}. These values of f, B_0, and n_{01} are taken from the RBSP-B observations shown in Figure 1b. The parallel wavelength λ is chosen to make n_2 less than n_{01} and n_{02}. In this case $n_2 = 190.1$ cm^{-3}, $\kappa_1 = 2.59$ rad/km ($\lambda_{\perp_1} = 2.42$ km), $\gamma_1 = 4.23$ rad/km, $\kappa_2 = 1.73$ rad/km ($\lambda_{\perp_2}$ $= 2.43$ km), and $\gamma_2 = 0.59$ rad/km.

For comparison, Figures 2d, 2e, and 2f show $E_x(x)$, $E_y(x)$, $E_z(x)$ for the wave with $f = 450$ Hz and $\lambda_\parallel = 49.5$ km in the magnetic field $B_0 = 437.8$ nT and the plasma with $n_{01} = 695.5$ cm^{-3} and $n_{02} = 100.0$ cm^{-3}. In this case, $n_2 = 84.5$ cm^{-3}, $\kappa_1 = 1.73$ rad/km ($\lambda_{\perp_1} = 3.63$ km), $\gamma_1 = 4.65$ rad/km, $\kappa_2 = 1.73$ rad/km ($\lambda_{\perp_2} = 3.64$ km), and $\gamma_2 = 0.74$ rad/km.

To verify that these waves propagate along the ambient magnetic field in a form of a localized wave package, we run time-dependent, two-dimensional simulations of the entire model (2)-(4). The numerical algorithm used in this study is based on the finite-difference, time-domain (FDTD) implementation of equations (2)-(4) in a two-dimensional rectangular domain [*Streltsov et al.*, 2006]. The size of the domain in the z direction is l_z (from $-l_z/2$ to $l_z/2$), and the size in the x direction is l_x (from $-l_x/2$ to $l_x/2$). The boundary conditions in the z-direction are periodic, and l_z is set equal to one parallel wavelength of the simulated wave, $\lambda_|$. The values of ($\mathbf{E}$, $\mathbf{B}$, and $\mathbf{v}$) are set equal to zero on the boundaries in the x direction (the Dirichlet boundary conditions). Simulations start from the initial conditions for $\mathbf{E}$, $\mathbf{B}$, and $\mathbf{v}$.

3 Numerical Results

Figure 3 shows results from the simulations of the whistler-mode waves with the parallel wavelength $\lambda_{\parallel} = 33.0$ km propagating in the uniform magnetic field with a magnitude $B_0 = 437.8$ nT. Initial conditions for the simulations were calculated from equations (17), (16), and (15) for the wave with the frequency $f = 450$ Hz. For these values of f, B_0, and $\lambda_{\parallel}$, the critical value of the plasma density defined by (7) is $n_2 = 190.1$ cm^{-3}.

Figure 3a shows the dynamics of E_y $(x,\, z = 0,\, t)$ in the simulation when the plasma density has a discontinuity at $x = 0$: $n = 695.5$ cm^{-3} when $x < 0$, and $n = 200.0$ cm^{-3} when $x \geq 0$. The frequency of the wave observed in this simulation is 447.4 Hz (which is close to the assumed frequency of 450 Hz). For $f = 447.4$ Hz, $\lambda_{\parallel} = 33.0$ km, and $B_0 = 437.8$ nT relation (7) provides $n_2 = 192.3$ cm^{-3}. The minimal density in the entire domain is larger than n_2, and hence, the wave is evanescent in the x direction. Relation (6) gives $\kappa_1 = 2.59$ rad/km, $\gamma_1 = 4.23$ rad/km, $\kappa_2 = 2.59$ rad/km, and $\gamma_2 = 0.59$ rad/km. Figures 2d - 2f show profiles of $E_x(x)$, $E_y(x)$, and $E_z(x)$ used in the simulations as the initial conditions. The simulation shows the wave dynamics during 0.1111 s corresponding to ≈ 50 periods of the wave with $f = 450$ Hz. Figure 3a' shows the density profile across $\mathbf{B}_0$ and the plot of $E_y(x, z = 0)$ in time $t = 0.0556$ s (near 25 wave period), and Figure 3a" shows the dynamics of E_y at the center of the computational domain, $E_y(x = 0, z = 0, t)$. The main conclusion from the plots shown in Figures 3a, 3a', and 3a" is that the VLF whistler-mode wave can indeed be guided along the ambient magnetic field by the discontinuity of the plasma density.

Figure 3b shows the dynamics of E_y $(x,\, z = 0,\, t)$ in the simulation when the plasma density has a finite ($\Delta x = 600$ m or $\approx(1/4)\ 2\pi/\kappa_2$) transition layer between two uniform regions. Within this layer, the magnitude of the plasma density changes linearly from 695.5 cm^{-3} to 200.0 cm^{-3}. The simulation starts from the same initial conditions as in the previously considered case of the plasma with a density discontinuity. These initial conditions are not the exact solution of the wave propagating in the plasma with a finite transition layer, and the numerical algorithm produces waves with a different frequency.

This happens because ω is connected to $k_{\parallel}$ and $k_{\perp}$ via the wave dispersion relation, and the algorithm controls only $k_{\parallel}$ via the boundary conditions in the z direction. Therefore, if the initial conditions do not match exactly the perpendicular structure of the wave propagating along the ambient magnetic field in the plasma with a finite transition layer, then the frequency of the obtained waves should be different from the frequency of the waves used to calculate the initial conditions.

In this case, simulation produces the waves with the frequency 436.7 Hz. For this frequency and $\lambda_{\|} = 33.0$ km, relation (7) gives the critical value of the density $n_2 = 201.8$ cm^{-3}. This value is larger than n_{02}, and hence, the wave with such f and $\lambda_{\|}$ can propagate across the ambient magnetic field in the x ¿ 0 part of the domain, where $n = 200$ cm^{-3}. The dynamic of VLF whistler-mode waves shown in Figures 3b - 3b" confirm this scenario.

Figure 3c shows the dynamics of E_y $(x,\, z = 0,\, t)$ in the simulation when the plasma density inside the entire domain is uniform, $n = 200$ cm^{-3}. The initial condition for this simulation again is calculated from the equations (17), (16), and (15) for the wave with a frequency 450 Hz localized in the x direction. Because these initial conditions do not represent the exact solution of the problem in the homogeneous plasma, the code produces the waves with a different frequency. Namely, in this case, the frequency of the obtained waves is 438.6 Hz. For this frequency and $\lambda_{\|} = 33.0$ km, relation (7) gives the critical value of the density $n_2 = 200.1$ cm^{-3}. This value is very close (it is larger by 0.05%) to the magnitude of the plasma density in the domain, and the resulting wave is very close to a so-called Gendrin's mode [*Gendrin*, 1961], which is a special case of VLF waves. The main feature of the Gendrin waves is that they have a real $k_\perp = k_{\|}((\omega_{ce}/2\omega)^2 - 1)^{1/2}$ (it is obtained from (6) when $n = n_2$), but the perpendicular component of their group velocity is equal to zero. Therefore, these waves carry their energy along the ambient magnetic field. The fact that Figure 3c shows some "spreading" of these waves across the magnetic field is due to the diffraction of the waves propagating from a localized source.

Now, let us consider the propagation of waves with $\lambda_{\|} = 49.5$ km. Figure 4 shows results from the simulations of the whistler-mode wave with $\lambda_{\|} = 49.5$ km in the uniform magnetic field $B_0 = 437.8$ nT. Figure 4a shows the dynamics of E_y $(x,\, z = 0,\, t)$ in the simulation where the plasma density has a narrow ($\Delta x = 100$ m) transition layer between the two regions with $n_{01} = 695.5$ cm^{-3} and $n_{02} = 100.0$ cm^{-3}. In the transition layer, the density changes linearly from 695.5 cm^{-3} to 100.0 cm^{-3} over the distance of 100 m, which is much less than the characteristic perpendicular size of the waves in both media ($2\pi/\kappa_{1,2} \approx 3.6$ km).

The initial conditions for the simulations were calculated using equations (17), (16) and (15) for the wave with f = 450 Hz in the plasma with a density discontinuity at x = 0. The profiles of the initial $E_x(x)$, $E_y(x)$, and $E_z(x)$ used in this simulation are shown in Figures 2d - 2f. However, because these initial conditions are not the exact solutions of the problem with a finite transition region, the frequency of the waves obtained in the simulations is not 450 Hz, but 444.4 Hz. For that frequency, B_0, and $\lambda_{\|}$, relation (7) gives the critical value of the density n_2 = 86.6 cm^{-3}. This value is less than the minimal density magnitudes in the entire domain. Therefore, the wave with these parameters will not propagate perpendicular to the background magnetic field, and, hence, it will be guided along the ambient magnetic field by this density gradient. Results from the simulation illustrated in Figures 4a - 4a" confirm this prediction.

Figure 4b shows the dynamics of E_y (x, z = 0, t) in the simulation where the plasma density has a wider (Δx = 1400 m) transition layer between the two regions with n_{01} = 695.5 cm^{-3} and n_{02} = 100.0 cm^{-3}. In this layer, the density changes linearly from 695.5 cm^{-3} to 100.0 cm^{-3}. The initial conditions for this simulation were calculated using equations (17), (16) and (15) for the wave with the frequency of 450 Hz in the plasma with a density discontinuity at x = 0 (see Figures 2d - 2f). However, because these initial conditions are not the exact solutions of the problem with the transition layer, and now the size of the layer is $\approx (1/3)2\pi/\kappa_{1,2}$, the frequency of the waves obtained in the simulations is not 450 Hz, but 395.3 Hz. For that frequency, B_0, and $\lambda_{\|}$, relation (7) gives the critical value of the density n_2 = 109.45 cm^{-3}. This value is larger than the density magnitude in the region on the right of the transition layer (100 cm^{-3}), and hence, the perpendicular wave number in that region is real, and the wave with these f and $\lambda_{\|}$ can propagate across the ambient magnetic field in that region. Results from the simulation shown in Figure 4b - 4b" confirm these speculations.

Finally, Figure 4c shows the dynamics of $E_y(x, z = 0, t)$ in the simulations with the uniform plasma density in the entire domain, n = 100 cm^{-3}. The initial conditions for this simulation were also calculated using equations (17), (16), and (15) for the wave with the frequency of 450 Hz. Because these initial conditions are not the exact solutions of the problem in the homogeneous media, the frequency of the waves obtained in the simulations is not 450 Hz, but 414.1 Hz. For this frequency, B_0, and $\lambda_{\|}$, relation (7) gives the critical value of the density n_2 = 99.8 cm^{-3}, whose value is almost equal to the density magnitude in the domain, and this wave is close to the Gendrin mode, considered in the case illustrated in Figure 3c. This wave has a real perpendicular wavenumber but its perpendicular component of the group velocity is equal to zero. So the wave is supposed to carry its electromagnetic power mostly along the ambient magnetic field, and "spreading" of the wave in the perpendicular direction is mostly attributed to the diffraction of the wave emitted by the finite source.

4 Discussion and Conclusions

The main goal of this study is to demonstrate that a single localized transverse inhomogeneity of the background plasma can guide a whistler-mode wave along the ambient magnetic field. It is motivated by the observations from the Van Allen Probes satellites revealing a large number of localized packages of VLF waves inside/near density gradients in the equatorial magnetosphere.

A similar task was undertaken by *Streltsov et al.* [2006]. These authors consider the guiding of the whittler-mode waves by the density gradient with a characteristic size larger than the perpendicular wavelength of the guided wave. They interpreted such a "broad" gradient as a combination of low-density and high-density ducts and show that it can guide waves with real $k_\parallel$ and $k_\perp$. They also showed that this ducting mechanism stops working when the perpendicular wavelength is comparable or less than the characteristic size of the density inhomogeneity.

In this paper, we consider the opposite limit, namely, the situation when the whistler-mode waves are guided along the magnetic field by transverse density gradients with a size much less then the characteristic perpendicular size of the wave. We are looking for the waves with a complex perpendicular wavenumber, which cannot propagate in the perpendicular direction. In a more general sense, we are looking for the solutions of this problem in the form of so-called surface waves, which are the waves propagating along the narrow boundary separating two medias with different parameters.

Mathematically, the perpendicular structure of these waves is described as a solution of equations (13) - (15) localized in the vicinity of the density gradient. We consider the simplest form of such solutions, appearing in the case of the sharp discontinuity in plasma density. We found an analytical solution describing corresponding surface waves, and we confirm with the numerical simulations of the entire EMHD model (2)-(4) that these waves are indeed guided by the discontinuity.

Simulations reveal that the parameters of the guided waves (frequency and the parallel wavelength) relate to the parameters of the plasma. And, similar to the cases of the waves guided by the high-density ducts (e.g., *Streltsov* [2021a]), the waves with some particular frequency and a parallel wavelength can be guided by the same gradient with less "leakage" than the others.

Simulations show that the quality of the wave trapping by a single gradient decreases with the increasing of the width of the transition region between the homogeneous parts. But we think that this happens because the initial conditions for simulations were set assuming that the width of this layer is equal to zero. Therefore, results of simulations can be quite different if these initial conditions are chosen as an appropriate solution of equations (13) - (15) for the case of a finite transition layer. We leave this problem for future studies.

Acknowledgments

This research was supported by the Air Force Office of Sponsored Research Grants FA9550-19-1-0052 and FA9453-21-2-0039. RBSP EMFISIS data are available from the University of Iowa (https://emfisis.physics.uiowa.edu/) and NASA CDAWeb (https://cdaweb.gsfc.nasa.gov/index.html/)

References

Chen, R., X. Gao, Q. Lu, L. Chen, B. Tsurutani, W. Li, N. Binbin, and S. Wang (2021a), In situ observations of whistler-mode chorus waves guided by density ducts., *J. Geophys. Res.: Soace Phys.*, *126*, doi:10.1029/2020JA028814.

Chen, R., X. Gao, Q. Lu, B. Tsurutani, and S. Wang (2021b), Observational evidence for whistler mode waves guided/ducted by the inner and outer edges of the plasmapause, *Geophys. Res. Lett.*, *48*, e2021GL092,652, doi: 10.1029/2021GL092652.

Gendrin, R. (1961), Le guidage des whistlers par le champ magnetique, *Planet. Space Sci.*, *5*(4), 274–282, doi:https://doi.org/10.1016/0032-0633(61)90096-4.

Gordeev, A., A. Kingsep, and L. Rudakov (1994), Electron magnetohydrodynamics, *Physics Reports*, *243*, 215–315.

Helliwell, R. (1965), *Whistlers and Related Ionospheric Phenomena*, Stanford University Press, Stanford.

Inan, U., and T. Bell (1977), The plasmapause as a VLF wave guide, *J. Geophys. Res.*, *82*, 2819.

Ke, Y., L. Chen, X. Gao, Q. Lu, X. Wang, R. Chen, H. Chen, and S. Wang (2021), Whistler-mode waves trapped by density irregularities in the earth's magnetosphere, *Geophys. Res. Lett.*, *48*, doi:10.1029/2020GL092305.

Kletzing, C., W. Kurth, M. Acuna, R. MacDowall, R. Torbert, T. Averkamp, D. Bodet, S. Bounds, M. Chutter, and J. Connerney (2013), The electric and magnetic field instrument suite and integrated science (EMFISIS) on RBSP, *The Van Allen Probes Mission*, pp. 127–181.

Kondrat'ev, I. G., A. V. Kudrin, and T. M. Zaboronkova (1999), *Electrodynamics of density ducts in magnetized plasmas*, Gordon and Breach, Amsterdam.

Sazhin, S. (1993), *Whistler-mode waves in a hot plasma*, Cambridge University Press, Cambridge.

Streltsov, A. (2021a), Whistlers in the Plasmasphere, *J. Geophys. Res.: Space Phys.*, *126*, doi:10.1029/2020JA028933.

Streltsov, A. (2021b), Whistler on a Shelf, *J. Geophys. Res.: Space Phys.*, *126*, e2021JA029,403, doi:10.1029/2021JA029403.

Streltsov, A. V., M. Lampe, W. Manheimer, G. Ganguli, and G. Joyce (2006), Whistler propagation in inhomogeneous plasma, *J. Geophys. Res.*, *111*, doi: 10.1029/2005JA011357.

Woodroffe, J., and A. Streltsov (2013), Whistler propagation in the plasmapause, *J. Geophys. Res.*, *118*, 716, doi:10.1002/jgra.50135.

Wygant, J., J. Bonnel, K. Goetz, R. Ergun, R. Mozer, S. Bale, M. Ludlam, P. Turin, P. Harvey, and R. Hochmann (2013), The electric field and waves instruments on the Radiation Belts Storm Probes mission, *Space Sci. Rev.*, *179(1-4)*, 183.

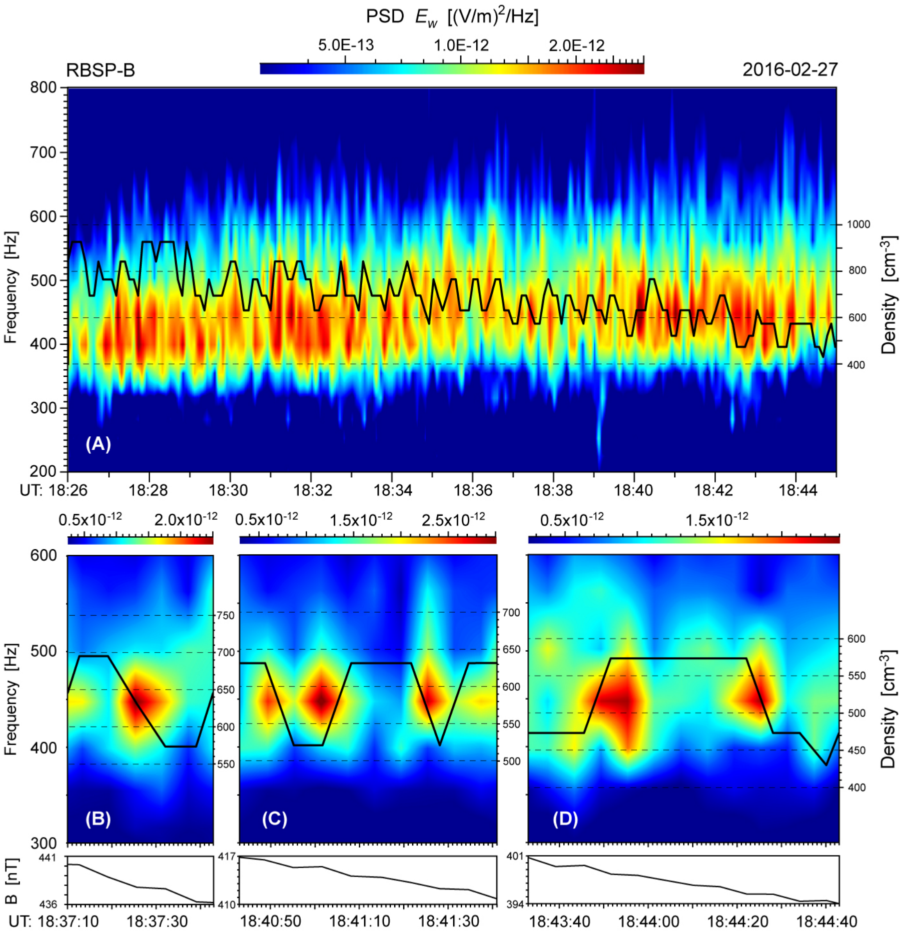

Figure 1. (A) Plasma density (black line) and the power spectral density (PSD) of E_w electric field observed by the RBSP-B satellite in the equatorial magnetosphere on 2016-02-27. Panels (B), (C), and (D) show four events of whistler-mode waves located on the isolated density gradients.

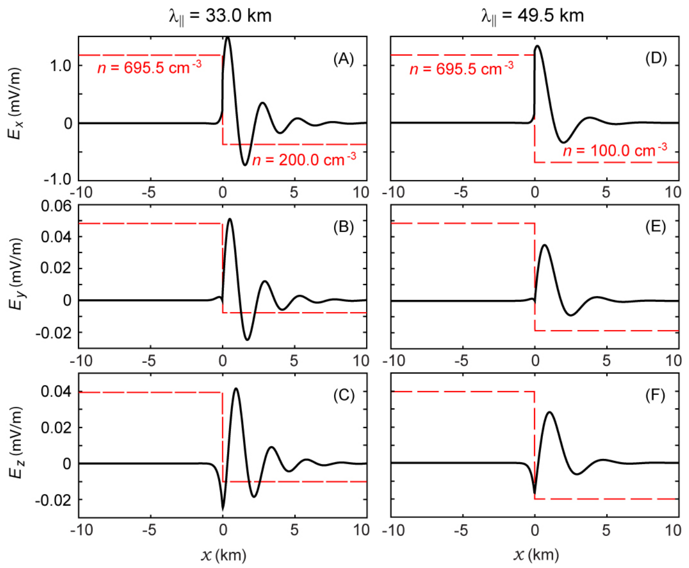

Figure 2. Panels (A), (B), and (C) show $E_x(x)$, $E_y(x)$, and $E_z(x)$ obtained from equations (15), (16), and (17) for $f = 450$ Hz, $\lambda_\parallel = 33$ km, $B_0 = 437.8$ nT, and the density profile shown with the red dashed line. Panels (D), (E), and (F) show $E_x(x)$, $E_y(x)$, and $E_z(x)$ for $f = 450$ Hz, $\lambda_\parallel = 49.5$ km, $B_0 = 437.8$ nT, and the density profile shown with the red dashed line.

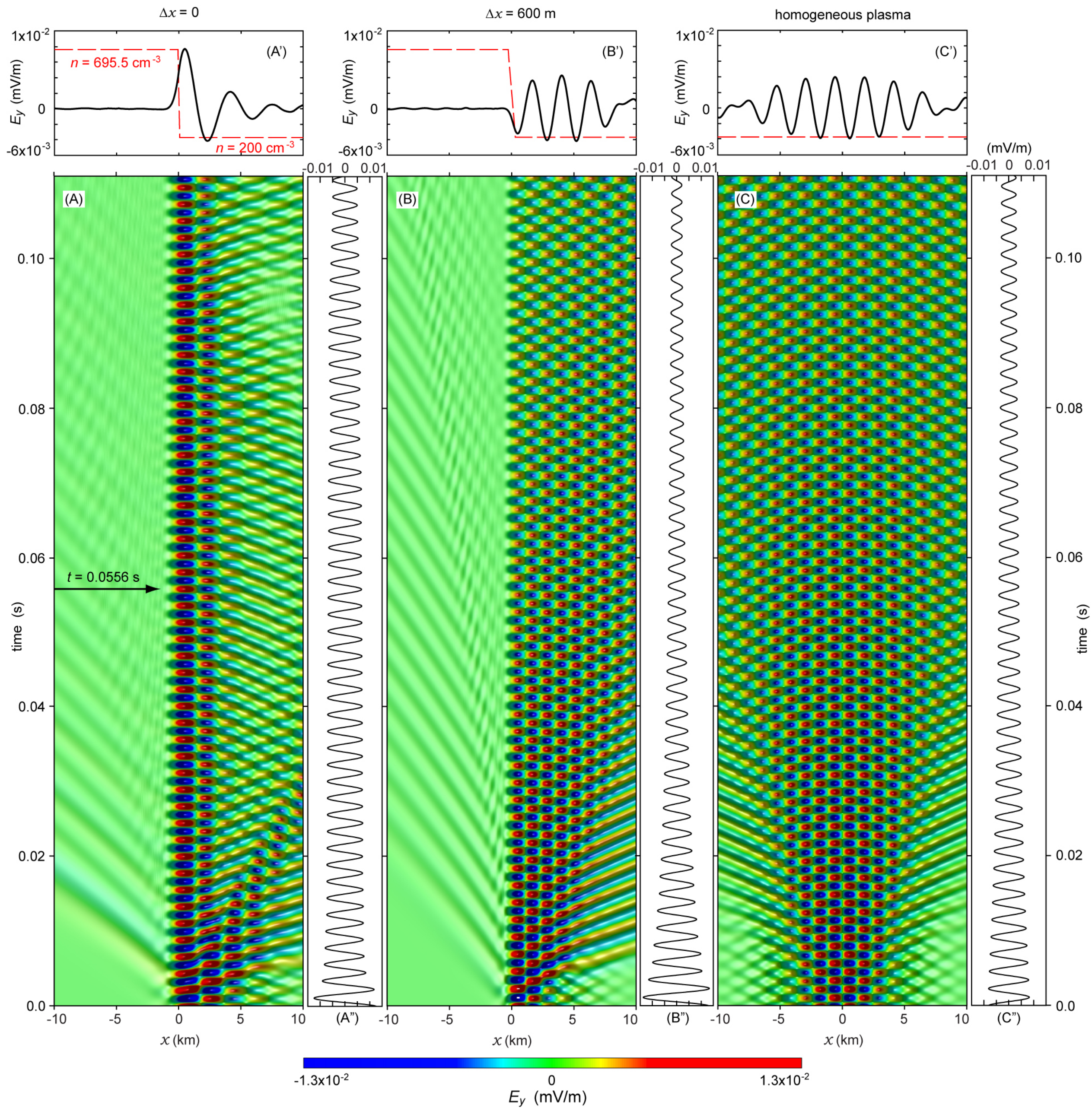

350 **Figure 3.** (A) Dynamics of E_y $(x, z = 0, t)$ in the simulation with $\lambda_\parallel = 33.0$ km, $B_0 = 437.8$ nT, and the density discontinuity at $x = 0$. (A') Density profile across $\mathbf{B}_0$ and the plot of E_y $(x, z = 0)$ in time $t = 0.0556$ s. (A") Dynamics of E_y at the center of the computational domain, E_y $(x = 0, z = 0, t)$. Panels (B), (B'), and (B") show results from the simulations with the same initial conditions as in the case (A) in the plasma with finite transition layer ($\Delta x = 600$ m) between two homogeneous regions. Panels (C), (C'), and (C") show results from the simulations with the same initial conditions as in the case (A) in the homogeneous plasma with density $n = 200$ cm^{-3}.

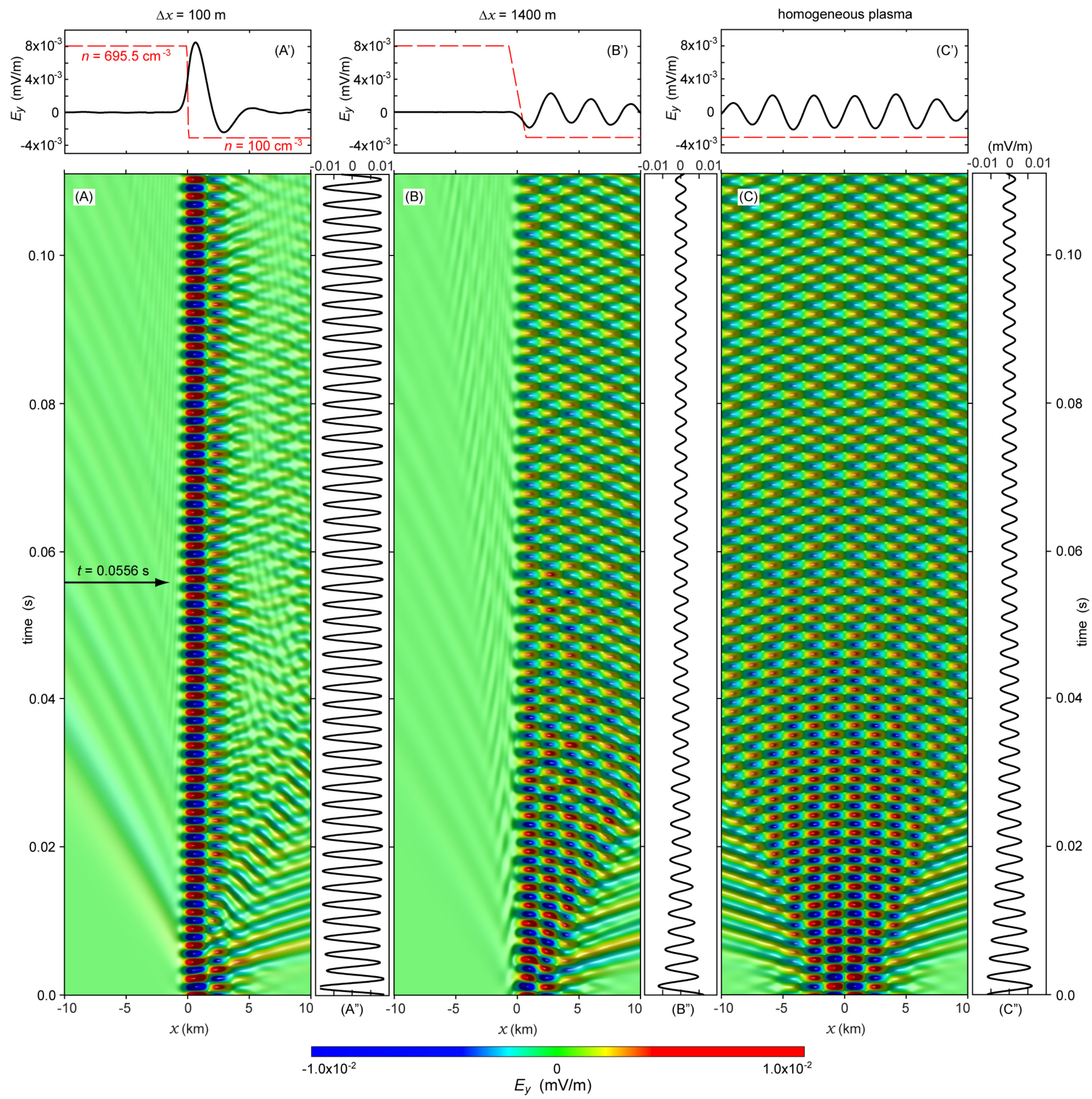

Figure 4. (A) Dynamics of E_y $(x, z = 0, t)$ in the simulation with $\lambda_{\|} = 49.5$ km, $B_0 = 437.8$ nT, and a narrow transition layer ($\Delta x = 100$ m) between two homogeneous density regions. (A') Density profile across $\mathbf{B}_0$ and the plot of E_y $(x, z = 0)$ in time $t = 0.0556$ s. (A") Dynamics of E_y at the center of the computational domain, E_y $(x = 0, z = 0, t)$. Panels (B), (B'), and (B") show results from the simulations with the same initial conditions as in the case (A) in the plasma with a broader transition layer ($\Delta x = 1400$ m) between two homogeneous regions. Panels (C), (C'), and (C") show results from the simulations with the same initial conditions as in the case (A) in the homogeneous plasma with density $n = 100$ cm^{-3}.